ISSN 1063-7842, Technical Physics, 2007, Vol. 52, No. 5, pp. 642–650. © Pleiades Publishing, Ltd., 2007.
Original Russian Text © V.I. Oreshkin, S.A. Barengol'ts, S.A. Chaikovsky, 2007, published in Zhurnal Tekhnicheskoĭ Fiziki, 2007, Vol. 77, No. 5, pp. 108–116.

EXPERIMENTAL INSTRUMENTS AND TECHNIQUES

Numerical Calculation of the Current Specific Action Integral at the Electrical Explosion of Wires

V. I. Oreshkin[a], S. A. Barengol'ts[b], and S. A. Chaikovsky[c]

[a] *Institute of High-Current Electronics, Siberian Division, Russian Academy of Sciences, Akademicheskiĭ pr. 2/3, Tomsk, 634055 Russia*

e-mail: oreshkin@ovpe.hcei.tsc.ru

[b] *Prokhorov General Physics Institute, Russian Academy of Sciences, ul. Vavilova 38, Moscow, 119333 Russia*

[c] *Lebedev Physics Institute, Russian Academy of Sciences, Leninskiĭ pr. 53, Moscow, 119991 Russia*

Received August 2, 2006

Abstract—The electrical explosion of aluminum wires is numerically simulated in the magnetohydrodynamic approximation for the current density ranging from 10^7 to 10^{10} A/cm^2 and times to explosion varying from 10^{-10} to 10^{-6} s. It is shown that, at current densities of 10^8–10^9 A/cm^2, low-temperature explosion conditions change to high-temperature ones, when inertial forces preventing the wire dispersion play a decisive role. This transition is accompanied by a sharp change in the thermodynamic parameters (the temperature and the energy deposited into the wire by the instant of explosion increase by several times), and the action integral for this transition increases smoothly approximately threefold as the explosion characteristics (current density and time to explosion) change by two orders of magnitude. The instant of transition from the low-temperature explosion to the high-temperature one depends on the radial dimensions of an exploding wire and does not depend on the properties of the environment.

PACS numbers: 52.80.Qj

DOI: 10.1134/S1063784207050179

INTRODUCTION

The wire (wire) electrical explosion (WEE) has long attracted the attention of researchers [1]. On the one hand, exploding wires are widely used in different applications, specifically, in missile technology to ignite a propellant [2], in high-voltage pulse techniques to concentrate the electric power [3], in the production of nanopowders [4], and in the fabrication of soft X-ray powerful sources for multiwire liners [5–7]. WEE implies a drastic change in the physical state of the metal as a result of intense energy liberation when high-density current pulses are applied to it. The exploding metal passes through all the states: from the condensed state to the gas plasma. From the fundamental standpoint, WEE is a suitable object for studying the thermophysical and transport properties of a dense nonideal plasma [8,9], in particular, for studying the metal conductivity near the critical point, i.e., the point on the phase diagram at which the liquid, gas-plasma, and two-phase domains meet.

The WEE process is closely related to pulsed breakdown in a vacuum, during which microtips on the cathode surface explode under the action of the field-emission current. As a result of this explosion, the cathode material passes into the plasma state, which causes explosive electron emission [10]. The criterion for pulsed breakdown between the needle-like cathode and plane anode in a vacuum has the form [11]

$$j^2\tau_{br} = \text{const}, \quad (1)$$

where j is the field-emission current density and τ_{br} is the delay time of field emitter breakdown. Relationship (1) is closely related with one of the WEE parameters—the integral of specific current action, h, used for description of the WEE process in terms of the similarity theory [12]. In addition, in the theory of vacuum breakdown, the specific action is the most important parameter of the ecton model in which the functioning of an emission center is described using similarity methods.

If metal conductivity σ depends only on the energy density introduced into the wire, ε_w, the integral of specific current action is given by

$$h = \int_{t_0}^{t} j^2 dt = \int_{\varepsilon_0}^{\varepsilon_w} \sigma(\varepsilon_w) d\varepsilon_w. \quad (2)$$

WEE is usually described by two types of the specific action integral [11]: h_1, the specific action from room temperature to the melting point, and h_2, the specific action from melting to explosion. If specific action h_1 for a given substance can be taken to be a constant with a good accuracy, specific action h_2 depends on the current density through the wire. This dependence can be caused both by the nonuniform heating of the wire and by the different dynamics of metal dispersion under different WEE conditions.

The specific action integral of current can be found in several ways [11, 13] both experimentally and theoretically. The specific actions were experimentally determined at current densities through the wire of 10^7–10^8 A/cm^2 for wires with a diameter of up to 10 μm. However, the explosion of wires with a diameter of about 1 μm at a current density of ~10^9 A/cm^2 and a time to explosion of 10^{-10}–10^{-9} s are of most interest for studies of the ecton process in a vacuum discharge. Nowadays, experimental studies of WEE under such conditions seem to be unfeasible; however, numerical calculations can well be carried out. To do this, it is necessary to have a reliable (experimentally verified) computer program that adequately describes main processes attendant on WEE.

The aim of this paper is numerical investigation into the electrical explosion of aluminum wires at a current density of ~10^9 A/cm^2 and a time to explosion of 10^{-10}–10^{-9} s. Such an object of investigation is due to the fact the thermophysical and transport properties of aluminum have been studied most thoroughly.

MAGNETOHYDRODYNAMIC MODEL

The processes accompanying the WEE process will be described in the magnetohydrodynamic (MHD) approximation. In this approximation, numerical simulation needs a knowledge of the equations of state over a wide range of thermodynamic parameters, as well as of the transport coefficients, among which the electrical conductivity is the most important. The WEE was simulated in the single-temperature MHD approximation, in which case the relevant equations in the case of the cylindrical geometry are

$$\frac{d\rho}{dt} + \frac{\rho}{r}\frac{\partial v}{\partial r} = 0, \tag{3}$$

$$\rho\frac{dv}{dt} = -\frac{\partial p}{\partial r} - j_z B_\varphi, \tag{4}$$

$$\rho\frac{d\varepsilon}{dt} = -\frac{p}{r}\frac{\partial v}{\partial r} + \frac{j_z^2}{\sigma} + \frac{1}{r}\frac{\partial}{\partial r}\left(\kappa\frac{\partial T}{\partial r}\right), \tag{5}$$

$$\frac{1}{c}\frac{\partial B_\varphi}{\partial t} = \frac{\partial E_z}{\partial r}; \quad j_z = \frac{c}{4\pi r}\frac{\partial (rB_\varphi)}{\partial r}, \tag{6}$$

$$j_z = \sigma E_z, \tag{7}$$

$$\varepsilon = f(\rho, T); \quad p = f(\rho, T). \tag{8}$$

Here, $\frac{d}{dt} = \frac{\partial}{\partial t} + v\frac{\partial}{\partial r}$ is the substantial derivative; ρ and T are the density and temperature of the material, respectively; v is the velocity radial component; p and ε are the pressure and internal energy, respectively; B_φ is the azimuthal component of the magnetic field intensity; E_z is the axial component of the electric field intensity; j_z is the axial component of the current density; and κ and σ are the thermal conductivity and electrical conductivity, respectively.

Equations (3)–(8) were solved numerically using the EXWIRE one-dimensional MHD program [9, 14] written in the Lagrangian coordinates. The program solves hydrodynamic equations (3)–(5) with the explicit difference scheme named "cross" [15], which handles the so-called combined (linear plus quadratic) pseudoviscosity to calculate shock waves. Implicit difference schemes based on the successive sweep method [16] were used to solve Maxwell equations (6) complemented by Ohm's law (7) and the heat conduction equation. The boundary condition for the Maxwell equations was set in the form

$$B_\varphi(R) = \frac{2I}{cr_w}, \tag{9}$$

where r_w is the time-dependent outer radius of the wire and I is the current through the wire.

The system of MHD equations is closed by the equations of state (8). For the metal, the wide-range semiempiric equations of state were used [17]. They are based on the model [18] including melting and evaporation. The conductivity of aluminum was found from the tables [19] compiled by Desjarlais from Sandia National Labs (United States) on the basis of the model [20] modified for experimental data.

Earlier, the authors used the EXWIRE program to simulate experiments on wire explosion in water [9, 21]. Using the equations of state [17], together with the conductivity tables [19], we reached good agreement between the calculated and experimental data for all the WEE conditions (from microsecond to nanosecond times of explosion). This is demonstrated in Fig. 1 plotting the calculated and experimental current and voltage waveforms for one conditions of aluminum wire (15 μm in diameter) explosion in water.

The aim of the numerical experiments, the results of which are given below, was gaining insight into the essence of the electrical explosion process rather than mere simulation or interpretation of specific experimental results. Therefore, we refused to use the equations for the current generator circuit, thereby significantly cutting the number of WEE-characterizing parameters (such as the inductance of the generator, capacity of the capacitor bank, the charge voltage of the bank, and the wire length) and, accordingly, apprecia-

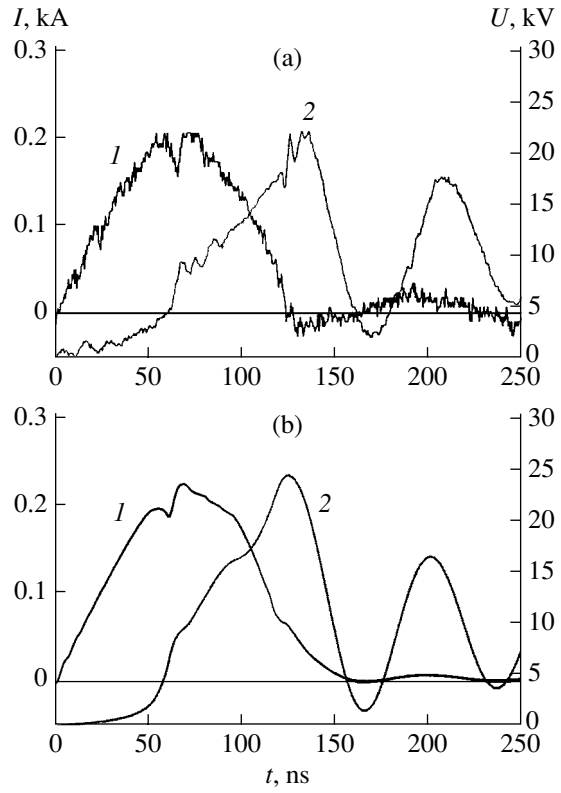

Fig. 1. (a) Experimental and (b) calculated waveforms of the (*1*) current and (*2*) voltage for the electrical explosion of an aluminum wire with a diameter of 15 μm and length of 2.6 cm in water.

bly simplifying the analysis of the results. It was assumed in the calculations that the current passing through the wire is a linearly increasing function of time,

$$I(t) = \pi r_0^2 \left(\frac{dj}{dt}\right) t, \tag{10}$$

where r_0 is the initial radius of the wire and $\left(\frac{dj}{dt}\right)$ is the rate of rise of the current density. The latter parameter was always taken to be a constant, varying from 2.5×10^{14} to 10^{20} A/(cm^2 s) in particular versions of calculation. In this way, we succeeded in simulating WEE conditions with a time to explosion varying from several submicroseconds to less than 100 ps.

RESULTS OF NUMERICAL SIMULATION

As has already been mentioned, there are several experimental and theoretical methods to find the specific action integral of current [11, 13]. The experimental methods [22, 23] do not, as a rule, take into account a change in the metal density during explosion, and the initial cross-sectional area of the wire is used in calculating the action integral. It is assumed that this change is so small that can be neglected. This assumption is obviously valid when the specific action integral is calculated from room temperature to the melting point (h_1); however, when the specific action integral is calculated from the melting point to the point of explosion (h_2), such an approach casts doubt.

In this paper, the current specific action integral was calculated as follows. First, the total action integral, $h = h_1 + h_2$, was calculated from room temperature to the point of explosion. Second, the integral was calculated by two ways. The first way is akin to the experimental method; i.e., a change in the cross-sectional area during WEE was not taken into account. Then, for the linearly increasing current, the current specific action integral is given by

$$h = \frac{1}{3}\left(\frac{dj}{dt}\right)^2 \tau_{ex}^3, \tag{11}$$

where τ_{ex} is the time to explosion. The second way of calculating the specific action integral takes into account a change in the cross-sectional area of the wire. In this case, when taking the integral in (2), one should average the value of j^2 over the cross-sectional area. This value can be averaged by a number of techniques, each yielding roughly identical results. When calculating the rms current density, we carried out averaging over the mass of the wire (which more correctly reflects the meaning of the action integral); i.e., the averaging was carried out in accordance with the expression

$$h^* = \frac{2\pi}{m}\int_0^{\tau_{ex}} dt \int_0^{r_w} r\rho j^2 dr, \tag{12}$$

where m is the linear mass of the wire.

One more uncertainty associated with the calculation of the current specific action is related to the inaccuracy of estimating the upper limit in integral (2), i.e., of determining the instance of explosion. Typical current and voltage waveforms are shown in Fig. 2a, and the time dependences of variously calculated current action integrals in Fig. 2b. Before melting, the time dependences of current specific actions $h(t)$ and $h^*(t)$ calculated by (11) and (12) at a variable upper limit of time integration are identical, as is seen from Fig. 2. These values start to diverge after melting (melting occurs between the 55th and 60th nanoseconds), when the expansion of the wire becomes appreciable. After melting, the discrepancy between $h(t)$ and $h^*(t)$ becomes essential. In other words, to calculate current specific action integral h_2 from melting to explosion, a change in the cross-sectional area of the wire should be taken into account; otherwise, this integral becomes overestimated. As to the upper limit of integration in (2), Fig. 2a shows that, when the current specific action is calculated according to (12), the upper limit is not as critical as when calculations are carried out by (11). Specific action $h^*(t)$ changes insignificantly with time

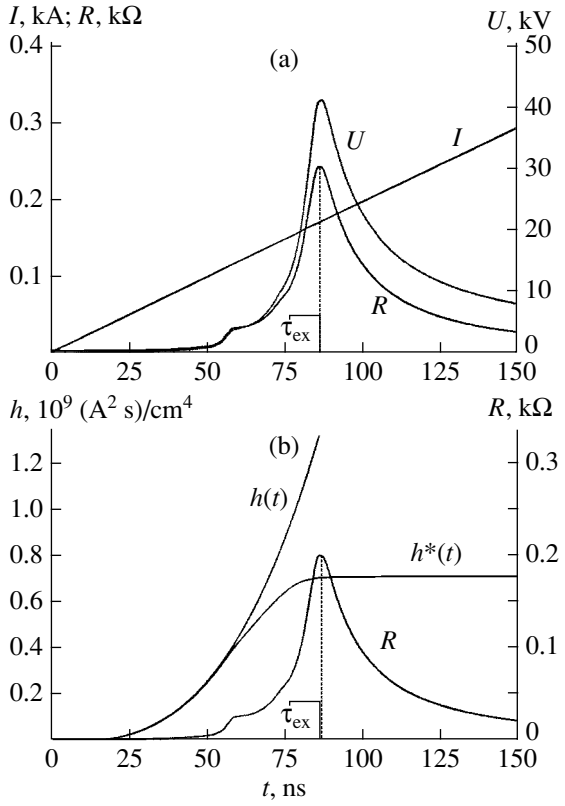

Fig. 2. (a) Current and voltage waveforms and (b) time dependences of the action integrals calculated without (h) and with (h^*) allowance for wire expansion, as well as the time dependence of the wire resistance (R) at the explosion of an aluminum wire of diameter 10 μm and length 1 cm for $\left(\frac{dj}{dt}\right) = 2.5 \times 10^{15}$ A/(cm^2 s).

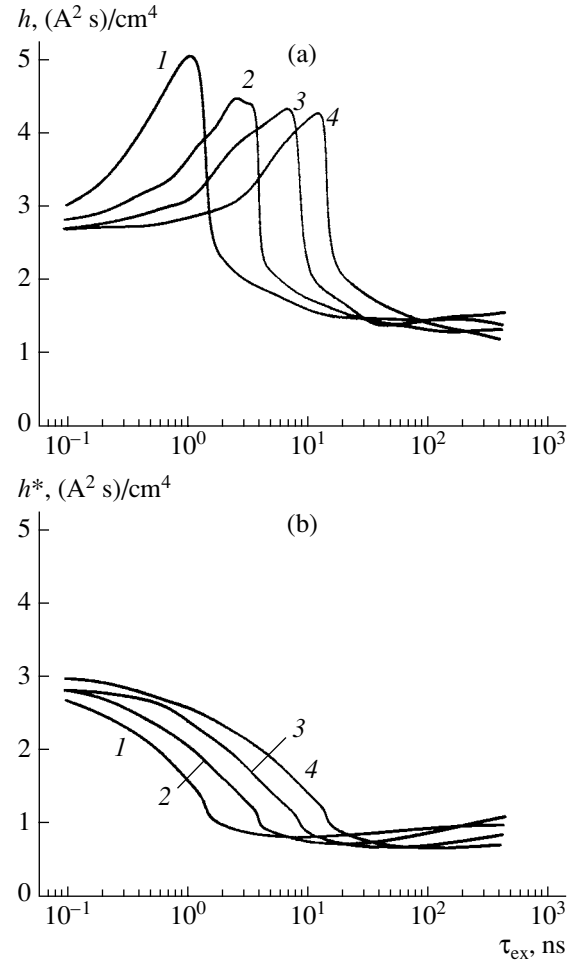

Fig. 3. Specific current action integrals (a) without (h) and (b) with (h^*) allowance for wire expansion vs. the time of explosion of an aluminum wire with a diameter of (*1*) 2, (*2*) 5, (*3*) 10, and (*4*) 20 μm in water.

from the instant of explosion (which in this case roughly equals 75 ns) to the maximum of the voltage and remains almost constant after explosion. In all the calculations, the results of which are given below, the time instant the resistance of the wire reaches a maximum is taken for the upper limit of integration, i.e., for instant of explosion τ_{ex}.

In the numerical calculations, we simulated the explosion of cylindrical aluminum wires with their diameter ranging from 2 to 20 μm. WEE was simulated in water and in a vacuum. For studying vacuum breakdown at the electrical explosion of a metal on the top of a microprotrusion [11], WEE in a vacuum is of most interest; in real experiments, however, WEE in a vacuum causes breakdown along the surface of the wire [24]. Such phenomena, i.e., surface breakdown, do not take place in the case of exploding microprotrusions, since the geometry of the problem changes in this case: at WEE, the current passes parallel to the surface of the wire, while at the explosion of microprotrusions, the current is normal to the surface of the exploding metal. Since WEE in a vacuum causes breakdown, all the available experimental values of the current action integral are related to explosions either in gases or in liquid insulators. The characteristics of WEE in liquid insulators differ slightly from those of WEE in gases, especially at gas elevated pressures. Therefore, the aim of WEE simulation in various media (water and vacuum) was to estimate the influence of the environment on the current specific action integral. Certainly, we did not take into account surface breakdown in our simulation.

Current specific action integrals h and h^* for WEE in water versus the time to explosion are shown in Fig. 3, and specific action integral h^* as a function of the time to explosion and current density is demonstrated in Figs. 4a and 4b, respectively. In the latter dependence, the current density was averaged over the mass of the wire and over time; i.e., the averaged current density was calculated from the expression

$$\langle j \rangle = \frac{2\pi}{m\tau_{ex}} \int_0^{\tau_{ex}} dt \int_0^{r_w} r\rho j dr. \qquad (13)$$

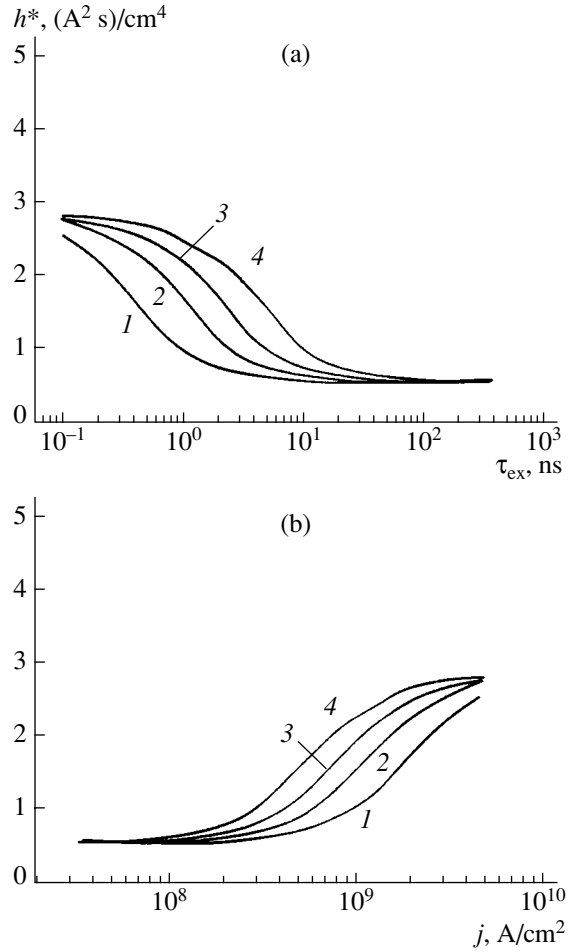

Fig. 4. Current specific action integral h^* as a function of the (a) time to explosion and (b) current density at the explosion of an aluminum wire with a diameter of (*1*) 2, (*2*) 5, (*3*) 10, and (*4*) 20 μm in a vacuum.

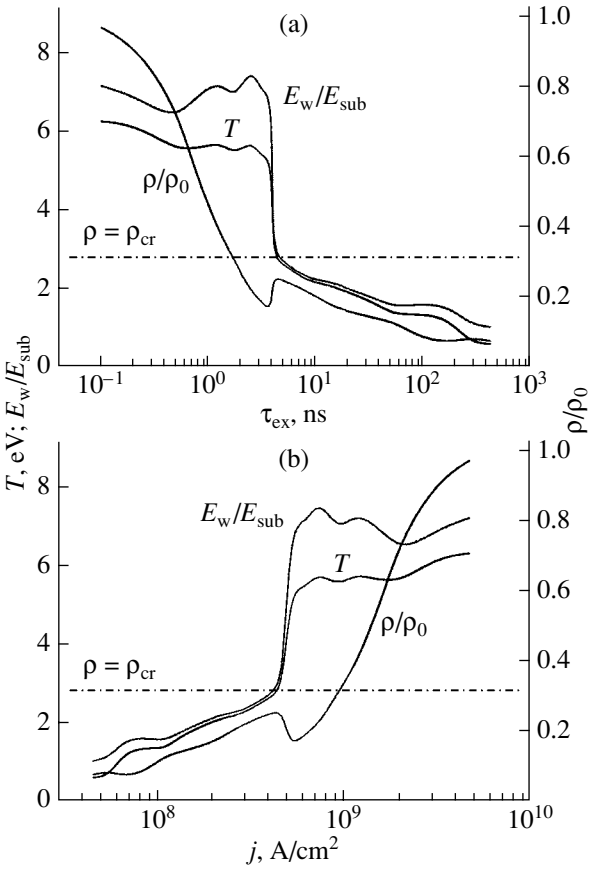

Fig. 5. Thermodynamic parameters of the metal vs. the (a) time to explosion and (b) current density at instant of explosion τ_{ex}. The diameter of the aluminum wire is 5 μm, WEE in water.

As is seen from Fig. 3a, when the time to explosion is more than 10 ns (or the current density is less than 10^8 A/cm^2), current action integral h slightly depends on the time to explosion (or on the current density) and size of the wire. For these times to explosion, the value of the integral is close to the values of h found experimentally for the explosion in gases without considering a change in the cross-sectional area of the wire. These values were about 0.9×10^9 (A^2 s)/cm^4 at a current density of ~10^7 A/cm^2 [23] and about 1.8×10^9 (A^2 s)/cm^4 at ~10^8 [11]. Current action integral h^* calculated with allowance for the wire expansion are 30–40% lower than integral h (Fig. 3); for the explosion in a vacuum, integrals h^* are 20–30% lower than for the explosion in water (Fig. 4).

The specific action integrals start growing at a current density of more than 10^8–10^9 A/cm^2 and, correspondingly, at an time to explosion less than 10 ns (Figs. 3, 4). The onset of growth depends on the radius of the exploding wire—for larger radius wires, the action integral starts to increase at lower current densities and at longer times to explosion—and does not depend on the properties of the medium in which the explosion occurs: if wires are equal in size, the action integrals begin to grow at the same times of explosion both in water and in a vacuum. This growth changes the thermodynamic parameters of the metal at the instant of explosion (the energy deposit into the wire, temperature, and density). This fact is demonstrated by Figs. 5 and 6, which show the dependences of the thermodynamic parameters for a wire of diameter 5 μm at the instant of explosion (it is remembered that the time the wire resistance reaches a maximum is taken for the instant of explosion). Plotted are temperature T, the ratio of energy deposit into the wire E_w to sublimation energy E_{sub} (i.e., to the energy needed for complete evaporation of the metal), and the ratio between the density of the metal ρ to its density under normal conditions ρ_0 (for aluminum $\rho_0 = 2.71$ g/cm^3). As is seen from these figures, if the expansion of the wire is taken into account, the growth of the current specific action integrals is rather smooth and the absolute value of the action integral increases approximately by three times

(in accordance with [11, 13]) as the explosion parameters (current density and time to explosion) change by two orders of magnitude. The growth of the action integrals is accompanied by a much sharper rise in the density of the metal at instant of explosion τ_{ex}; by an increase in the temperature to 5–6 eV; and, hence, by an increase in the energy deposited into the wire (it amounts to several sublimation energies). This rise is fast, especially for WEE in water; therefore, it can be argued that, with increasing the current density, low-temperature WEE conditions switch to high-temperature conditions, under which the energy deposit into the conductor several times exceeds the energy needed for complete evaporation of the metal.

RESULTS AND DISCUSSION

From the experimental data for WEE it is known that, as the rate of rise of the current increases, so does the energy deposit into the wire during the explosion [1, 24]. For long current rise times, when the current density through the wire far exceeds 10^8 A/cm^2, the energy deposit is several times higher than the metal sublimation energy, and not only for the explosion in a gas [22, 23] but also for the explosion in a vacuum [25]. Two reasons for such behavior of the material have been suggested in the literature. The first viewpoint is based on the assumption that the magnetic pressure [26] counterbalances the gaskinetic pressure and thereby makes the metal dispersion difficult. The second reason is the influence of inertial forces, which do not allow the wire to expand considerably for a short time [27]. The latter viewpoint has found the most convincing experimental [28, 29] and theoretical [30] confirmations, and our calculations count in favor of this hypothesis too.

Based on the assumption about the decisive role of inertial forces, let us estimate the size of the wire at which these forces influence the wire dispersion. It is well known [3] that, for moderate current densities, the wire explodes when its density is close to the density at the critical point, i.e., at the point on the metal phase diagram where the liquid, gas-plasma, and two-phase (vapor + condensate) domains meet. This can also be seen in Figs. 5 and 6, where the density at the critical point, ρ_{cr}, is shown by the dash-and-dot line. Critical density ρ_{cr} is usually three to five times smaller than normal density ρ_0. Hence, by the time of explosion, the wire expands approximately two times in the radial direction. Then, the time to explosion can be estimated as

$$\tau_{ex} \approx \frac{r_0}{v}, \tag{14}$$

where r_0 is the initial radius of the wire and v is the rate of its expansion. The latter parameter can be obtained from law of conservation of momentum (4) if electromagnetic forces are neglected and the values of the thermodynamic parameters involved in (4) are set equal to the values at the critical point,

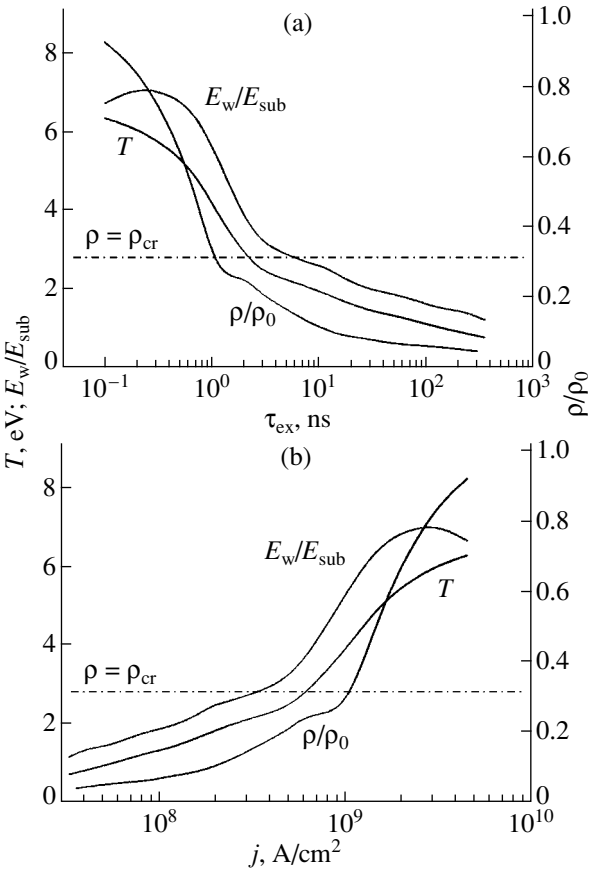

Fig. 6. The same as in Fig. 6 for WEE in a vacuum.

$$\rho_{cr}\frac{v}{\tau_{ex}} \approx \frac{p_{cr}}{r_0}, \tag{15}$$

where p_{cr} is the pressure at the critical point. Then, from (14) and (15), we can obtain the condition for the transition from the low to high temperature regime in terms of the wire radius and time to explosion,

$$r_0 < \tau_{ex}\sqrt{\frac{p_{cr}}{\rho_{cr}}}. \tag{16}$$

For aluminum, the parameter values at the critical point are p_{cr} = 4.45 kbar, ρ_{cr} = 0.855 g/cm^3, and T_{cr} = 0.55 eV. If these values of p_{cr} and ρ_{cr} are substituted into (16), we find that, for wires with a diameter of 2, 5, 10, and 20 μm, the time to explosion at which the transition to the high-temperature WEE regime occurs is 1.4, 3.5, 7.0, and 14.0 ns, respectively. This is in good agreement with the calculated dependences in Figs. 3–6.

Consider the position of the curve corresponding condition (16) on the WEE regime diagram (Fig. 7). The diagram is constructed according to Chace and Levine's classification of WEE conditions [31]. This

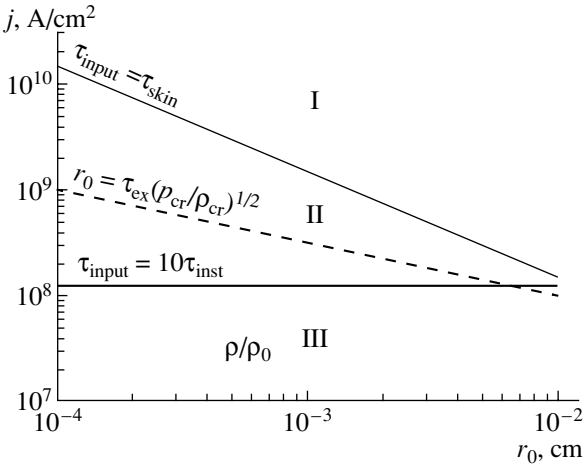

Fig. 7. WEE regime diagram: I, skin effect domain (ultrafast WEE); II, fast WEE; and III, slow WEE.

classification is based on the ratios of the times of different processes attendant on WEE. The basic time scales, which describe the overall WEE process, are the time to loss of metallic conduction (τ_{input}), time of MHD instability development (τ_{inst}), and time to skin effect appearance (τ_{skin}).

The time to loss of metallic conduction is determined from the ratio of the sublimation energy to the energy deposit due to Joule heating,

$$\tau_{input} = \frac{\rho \Lambda_i \sigma}{m_i j^2}, \quad (17)$$

where Λ_i is the sublimation energy per atom, ρ is the density of the metal, m_i is the atomic mass, and σ is the conductivity of the metal.

The time of development of sausage-type MHD instability (the mode $m = 0$) [32] depends on the wire radius and propagation velocity of MHD disturbances in the wire,

$$\tau_{inst} = \frac{r_0}{c_A} = \frac{r_0\sqrt{4\pi\rho}}{B_\varphi} = \frac{c\sqrt{\rho}}{\sqrt{\pi} j}, \quad (18)$$

where B_φ is the magnetic field intensity, $c_A = \dfrac{B_\varphi}{\sqrt{4\pi\rho}}$ is the Alfvén velocity [33], and c is the speed of light in a vacuum. In (18), the magnetic field intensity was taken to be equal to that on the wire surface according to (9).

The time to the skin effect is specified by magnetic field diffusion and depends on the radius and conductivity of the wire [33],

$$\tau_{skin} = \frac{4\pi r_0^2 \sigma}{c^2}. \quad (19)$$

If the typical time of MHD instability development is much shorter than the time to loss of metallic conduction ($\tau_{inst} \ll \tau_{input}$), the WEE process is slow; otherwise, we deal with the fast WEE process. For a tenfold difference in these times, we obtain from (17) and (18) that, for the fast process to set in, the current density must meet the condition

$$j > \frac{\sqrt{\pi\rho}\,\Lambda_i \sigma}{10 m_i c}. \quad (20)$$

Along with the slow and rapid WEE conditions, it is customary to separate out the ultrafast regime, when the magnetic field has no time to penetrate deep into the wire; i.e., the skin effect is observed and mainly surface layers of the wire heat up. This regime is achieved if the typical time to the skin effect is higher than the time to loss of metallic conduction ($\tau_{skin} > \tau_{input}$). In this case, from (17) and (19), we obtain

$$j > \frac{c}{2r_0}\sqrt{\frac{\rho\Lambda_i}{\pi m_i}}. \quad (21)$$

As follows from Fig. 7, the fast WEE regime for aluminum is realized at current densities of more than ~10^8 A/cm^2 and the ultrafast regime for micrometer wires is achieved at a current density higher than ~10^{10} A/cm^2.

Then, having related time to explosion τ_{ex} with the current density via the specific current action integral,

$$h \approx j^2 \tau_{ex}, \quad (22)$$

and having substituted (22) into (16), we arrive at

$$j < \sqrt{\frac{h}{r_0}\left(\frac{p_{cr}}{\rho_{cr}}\right)^{1/2}}. \quad (23)$$

When condition (23) is satisfied, inertial forces do not influence the wire dispersion at WEE and the low-temperature explosion regime sets in. Otherwise, inertial forces retard the wire dispersion and the energy deposit heating the material to temperatures of several electronvolts is necessary.

The dash-and-dot line in Fig. 7 corresponds to (23). This line splits the domain of fast WEE into two, low-temperature and high-temperature, subdomains.

To conclude this section, let us discuss the above results in terms of the ecton model of the cathode spot in a vacuum discharge [11]. This model is based on the emissive–resistive mechanism of cathode erosion. According to this mechanism, the cathode material is carried away due to intense Joule heating under the action of the emission current. The density of the emission current is high because of a high temperature on the emitting area. For example, calculations show that, early in the "operation" of an emission center at current densities of 10^9–10^{10} A/cm^2, the surface temperature reached several tens of thousands of degrees, while the cathode material was still in the condensed state because of the sluggishness of the erosion process [34].

This statement came under criticism: it was assumed that such a high energy deposit or, in other words, such a high temperature of the cathode in the condensed state is basically impossible. Our results indicate that the high-temperature regime sets in under these conditions. Therefore, at the initial stage of emission center operation, the energy deposit into the cathode indeed may raise the temperature to several tens of thousands of degrees. Such an increase in the temperature, in turn, provides a high density of the emission current.

The transition to the high-temperature explosion regime is accompanied by the growth of the specific action integral, unlike the prediction of the simplest ecton model (based on the similarity theory) that this integral is constant during the ecton process. However, in view of the fact that the time to explosion of micrometer wires is several nanoseconds under the high-temperature conditions (Fig. 4a) and that the duration of the ecton process is one order of magnitude longer, the assumption that the action integral is constant can be considered valid. The transition of WEE to the high-temperature regime influences ecton processes at their initial stage only.

CONCLUSIONS

Numerical simulation of the electrical explosion of aluminum wires shows that, at current densities through the wire of 10^8–10^9 A/cm^2, the low-temperature regime switches to the high-temperature one, when inertial forces preventing the wire dispersion play the decisive role. This transition is characterized by a sharp change in the thermodynamic parameters of the metal: the energy deposit into the wire becomes equal to several sublimation energies by the time to explosion and the plasma temperature reaches 6–8 eV. At this transition, the specific action integral calculated with allowance for wire expansion during the explosion increases smoothly approximately by three times as the explosion parameters (current density and time to explosion) change by two orders of magnitude. The instant of low-to-high temperature switching depends on the radius of the exploding wire and does not depend on the properties of the medium where the explosion takes place. The results obtained are in agreement with the basic ideas of the ecton model of a vacuum discharge and can be used in studying physical processes accompanying the initiation and evolution of an electrical discharge in a vacuum.

ACKNOWLEDGMENTS

We are grateful to G.A. Mesyats for problem definition and interest in this work. We also thank K.V. Khishchenko, P.R. Levashov, and M. Desjarlais for assistance.

This work was supported by the Russian Foundation for Basic Researchers (grant nos. 05-02-08351, 05-02-16845, and 05-02-08240-ofi_a) and the program "Basic Problems in High-Power Piko- and Nanoseconds Electronics."

V.I. Oreshkin is indebted to the Domestic Science Support Foundation.

REFERENCES

1. A. A. Rukhadze, *Exploding Wires* (Inostrannaya Literatura, Moscow, 1959) [in Russian].
2. W. G. Chace, Phys. Today **17** (8), 19 (1964), [Usp. Fiz. Nauk **85**, 381 (1965)].
3. V. A. Burtsev, N. V. Kalinin, and A. V. Luchinskiĭ, *Electrical Explosion of Wires and Its Application in Physical Equipment* (Energoizdat, Moscow, 1990) [in Russian].
4. Yu. A. Kotov and N. A. Yavorskiĭ, Fiz. Khim. Obrab. Mater., No. 4, 24 (1978).
5. V. E. Grabovskiĭ, O. Yu. Vorob'ev, K. S. Dyabilin, et al., Zh. Éksp. Teor. Fiz. **109**, 1 (1996) [JETP **82**, 445 (1996)].
6. S. A. Pikuz, T. A. Shelkovenko, J. B. Greenly, et al., Phys. Rev. Lett. **83**, 4313 (1999).
7. R. B. Spielman, C. Deeney, G. A. Chandler, et al., Phys. Plasmas **5**, 2105 (1998).
8. A. M. DeSilva and J. D. Katsouros, Phys. Rev. E **57**, 6557 (1998).
9. V. I. Oreshkin, R. B. Baksht, A. Yu. Labetsky, et al., Zh. Tekh. Fiz. **74** (7), 38 (2004) [Tech. Phys. **49**, 843 (2004)].
10. G. A. Mesyats and D. I. Proskurovskiĭ, Pis'ma Zh. Éksp. Teor. Fiz. **13**, 7 (1971) [JETP Lett. **13**, 4 (1971)].
11. G. A. Mesyats, *Ectons in Vacuum Discharge: Breakdown, Spark, and Arc* (Nauka, Moscow, 2000) [in Russian].
12. L. I. Sedov, *Similarity and Dimensional Methods in Mechanics* (Nauka, Moscow, 1981; Academic, New York, 1959).
13. G. A. Mesyats, *Pulsed Power* (Nauka, Moscow, 2004; Plenum, New York, 2005).
14. V. I. Oreshkin, V. S. Sedoy, and L. I. Chemezova, Prikl. Fiz., No. 3, 94 (2001).
15. N. N. Kalitkin, *Numerical Methods* (Nauka, Moscow, 1978) [in Russian].
16. A. A. Samarskiĭ and Yu. P. Popov, *Difference Schemes of Gas Dynamics* (Nauka, Moscow, 1980) [in Russian].
17. S. I. Tkachenko, K. V. Khishchenko, V. S. Vorob'ev, et al., Teplofiz. Vys. Temp. **39**, 728 (2001).
18. A. V. Bushman and V. E. Fortov, Sov. Technol. Rev. B Phys. **1**, 219 (1987).
19. M. P. Desjarlais, Contrib. Plasma Phys. **41**, 267 (2001).
20. Y. T. Lee and R. M. More, Phys. Fluids **27**, 1273 (1984).
21. A. G. Rousskikh, R. B. Baksht, V. I. Oreshkin, and A. V. Shishlov, in *Proceedings of the 5th International Conference on Dense Z-Pinches, Albuquerque, New Mexico (Melville, New York, AIP), 2002*, pp. 217–220.
22. L. I. Chemezova, G. A. Mesyats, V. S. Sedoy, et al., in *Proceedings of the 18th International Symposium on Discharges and Electrical Insulation in Vacuum (ISDEIV), Eindhoven, 1998*, pp. 48–51.
23. V. S. Sedoy, G. A. Mesyats, V. I. Oreshkin, et al., IEEE Trans. Plasma Sci. **27**, 845 (1999).

24. A. G. Rousskikh, R. B. Baksht, A. Yu. Labetsky, et al., Fiz. Plazmy **30**, 1 (2004) [Plasma Phys. Rep. **30**, 944 (2004)].
25. G. S. Sarkisov, S. E. Rosenthal, K. R. Cochrane, et al., Phys. Rev. E **71**, 046404 (2005).
26. V. I. Petrosyan and E. I. Dagman, Zh. Tekh. Fiz. **39**, 2084 (1969) [Sov. Phys. Tech. Phys. **14**, 1567 (1969)].
27. S. V. Lebedev and A. I. Savvatimskiĭ, Zh. Tekh. Fiz. **54**, 1794 (1984) [Sov. Phys. Tech. Phys. **29**, 1045 (1984)].
28. V. V. Ivanov, Teplofiz. Vys. Temp. **21**, 154 (1983).
29. V. S. Sedoy, Doctoral Dissertation (Tomsk, 2003).
30. Yu. A. Kotov, O. M. Samatov, V. S. Sedoy, et al., in *Megagauss Field and Pulsed Power Systems* (Nova Science, New York, 1990), pp. 497–502.
31. W. G. Chace and M. A. Levine, J. Appl. Phys. **31**, 1298 (1960).
32. K. B. Abramova, N. A. Zlatin, and B. P. Peregud, Zh. Éksp. Teor. Fiz. **69**, 2007 (1975) [Sov. Phys. JETP **42**, 1019 (1975)].
33. L. D. Landau and E. M. Lifshitz, *Course of Theoretical Physics*, Vol. 8: *Electrodynamics of Continuous Media* (Nauka, Moscow, 1982; Pergamon, New York, 1984).
34. E. A. Litvinov, G. A. Mesyats, and A. G. Parfenov, Dokl. Akad. Nauk SSSR **274**, 864 (1983) [Sov. Phys. Dokl. **28**, 272 (1983)].

Translated by M. Astrov